Local electronic structure of Mn dopants in ZnO probed by resonant inelastic x-ray scattering

2007 J. Phys.: Condens. Matter 19 276210

(http://iopscience.iop.org/0953-8984/19/27/276210)

IOP PUBLISHING JOURNAL OF PHYSICS: CONDENSED MATTER

J. Phys.: Condens. Matter **19** (2007) 276210 (8pp) doi:10.1088/0953-8984/19/27/276210

Local electronic structure of Mn dopants in ZnO probed by resonant inelastic x-ray scattering

G S Chang[1], E Z Kurmaev[2], S W Jung[3], H-J Kim[3], G-C Yi[3], S-I Lee[4], M V Yablonskikh[1,2], T M Pedersen[1], A Moewes[1] and L D Finkelstein[2]

[1] Department of Physics and Engineering Physics, University of Saskatchewan, 116 Science Place, Saskatoon, SK, S7N 5E2, Canada
[2] Institute of Metal Physics, Russian Academy of Sciences-Ural Division, Yekaterinburg, 620219, Russia
[3] National Creative Research Initiative Center for Semiconductor Nanorods and Department of Materials Science and Engineering, Pohang University of Science and Technology (POSTECH), Pohang 790-784, Korea
[4] NCRICS and Department of Physics, Pohang University of Science and Technology (POSTECH), Pohang 790-784, Korea

E-mail: gapsoo.chang@usask.ca (G S Chang)

Received 9 November 2006, in final form 4 June 2007
Published 21 June 2007
Online at stacks.iop.org/JPhysCM/19/276210

Abstract

The electronic structure of Mn dopants in ZnO epitaxial thin films synthesized at different temperatures has been investigated using resonant inelastic x-ray scattering. The resulting Mn $L_{2,3}$ x-ray emission spectra of $Zn_{0.8}Mn_{0.2}O$ (resonantly excited at L_2 and L_3 absorption edges) reveal different spectral features depending on the growth temperature of the films. The relative integral intensity ratio of Mn L_2 to Mn L_3 emission lines is greatly suppressed in the case of nonmagnetic $Zn_{0.8}Mn_{0.2}O$ grown at 700 °C due to $L_2L_3M_{4,5}$ Coster–Kronig transitions. The ferromagnetic sample grown at 600 °C exhibits a normal oxide structure. The results suggest that a high growth temperature causes direct Mn–Mn bonds from the segregation of Mn atoms in ZnO. Therefore the disappearance of ferromagnetism in Mn-doped ZnO can be attributed to antiferromagnetic Mn–Mn exchange interactions due to the inhomogeneous local environment around the Mn impurities.

1. Introduction

Ferromagnetism of diluted magnetic semiconductors (DMSs) with a high Curie temperature (T_C) has been extensively studied over the last 15 years, ever since ferromagnetic properties in Mn-doped III–V semiconductors ($Ga_{1-x}Mn_xAs$) were discovered at temperatures above 100 K [1]. Many theoretical approaches have been made to explain the magnetic and electric properties of these exotic systems and to ultimately propose new DMSs possessing a T_C

that is above room temperature (RT). ZnO has garnered special interest because this II–VI semiconductor with a wide band gap is piezoelectric and optically transparent for visible light, and thus can be widely applied to optoelectronic devices. According to the Zener model calculation done by Dietl *et al* [2], ferromagnetic properties above RT can be realized in DMSs with a wurtzite crystal structure, such as ZnO and GaN that contains 5% of Mn dopants and 3.5×10^{20} holes cm^{-3}. On the other hand, *ab initio* band calculations by Sato *et al* predict stable ferromagnetism in $Zn_{1-x}Mn_xO$ based on p-type ZnO and antiferromagnetism in the system with n-type carriers [3]. The same group also suggests that both carrier-undoped and n-type ZnO-based DMSs can attain ferromagnetism if Fe, Co, or Ni is used as a dopant instead of Mn [4].

However, one of the major problems hampering experimental development of ferromagnetic Mn-doped ZnO is the synthesis of a p-type ZnO-based compound. This is because the undoped ZnO-based compound usually shows n-type conduction and many types of dopants (B, Al, Ga, In, and F) are known as donors for ZnO [5, 6]. The p-type conduction in ZnO has only been reported via methods such as N doping and Ga–N codoping [7–9]. In the meantime, several papers have reported the induction of ferromagnetism in n-type ZnO doped with Mn contrary to theoretical calculations. When $Zn_{1-x}Mn_xO$ thin films are prepared under appropriate conditions (in terms of growth temperature and oxygen pressure), the films show ferromagnetic behaviour below and even up to RT [10–12]. Since the magnetism of Mn-doped ZnO correlates with the electronic exchange interactions of the Mn atom with its neighbouring atoms and also the surrounding carriers, the local electronic structure of the Mn dopants provides important information for understanding these unusual DMSs.

In the present study we employed soft x-ray emission spectroscopy (XES) to investigate the electronic structure of Mn dopants in n-type $Zn_{0.8}Mn_{0.2}O$ epitaxial thin films grown at different temperatures. Element-specific XES provides a powerful way to investigate changes in the local structure of magnetic dopants in DMSs because the involved x-ray transitions occur within the excited atom (Mn in our case), and are predominantly affected by the first coordination sphere. The resonant inelastic Mn $L_{2,3}$ soft x-ray scattering spectra of ferromagnetic n-type $Zn_{0.8}Mn_{0.2}O$ are compared to those of a nonmagnetic sample of the same stoichiometry. The change in the local environment of the Mn dopants depending on the growth temperature is also discussed.

2. Experimental details

High-quality epitaxial films of $Zn_{0.8}Mn_{0.2}O$ were grown on $Al_2O_3(0001)$ substrates in an ultra-high-vacuum chamber under a base pressure of mid-10^{-9} Torr. For the growth of $Zn_{0.8}Mn_{0.2}O$ films, a stoichiometric $Zn_{0.8}Mn_{0.2}O$ target was ablated by the third harmonics (wavelength of 355 nm) of a Nd:YAG laser as described elsewhere [10]. The pulse duration and fluence of the laser beam were 5 ns and 1 J cm^{-2}, respectively. During film growth, the substrates were heated to 600 and 700 °C using a pyrolytic boron nitride-coated ceramic heater. The magnetic measurements were carried out with a superconducting quantum interference device (SQUID). The temperature-dependent magnetization (M–T) curves from 5 to 200 K were measured at an applied field of 500 Oe and the magnetic hysteresis (M–H) curves at 5 K were recorded in the field range -6000 Oe $\leqslant H \leqslant$ 6000 Oe. X-ray diffraction (XRD) was employed to verify the crystal structure and orientation of the $Zn_{0.8}Mn_{0.2}O$ films.

Soft x-ray emission spectroscopy measurements were carried out at beamline 8.0.1 of the Advanced Light Source at Lawrence Berkeley National Laboratory. Resonant and nonresonant Mn $L_{2,3}$ (3d4s $\rightarrow$ 2p transition) emission spectra were recorded at RT. All measured spectra are normalized to the number of photons falling on the sample monitored by a highly transparent

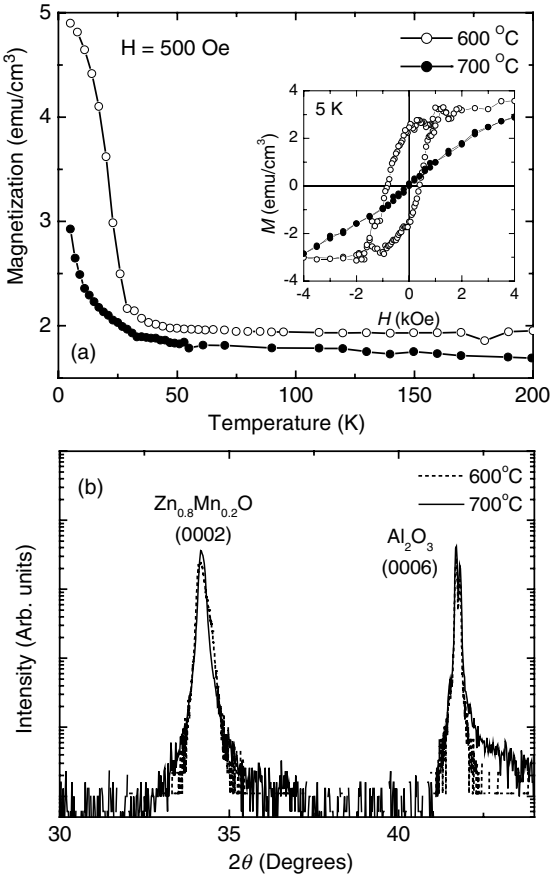

Figure 1. (a) M–T curves and (b) θ–2θ XRD patterns of $Zn_{0.8}Mn_{0.2}O$ films grown at 600 and 700 °C. The inset in (a) shows the M–H curves of corresponding samples.

gold mesh. In order to select the appropriate excitation energies for the resonant Mn $L_{2,3}$ emission, x-ray absorption spectra were recorded in the total electron yield (TEY) mode.

3. Results and discussion

Figure 1(a) shows the magnetic characteristics of the $Zn_{0.8}Mn_{0.2}O$ films investigated using a SQUID magnetometer. As shown in the M–T curves, the onset of ferromagnetic ordering is observed at 30 K for the $Zn_{0.8}Mn_{0.2}O$ film grown at 600 °C while both samples remain paramagnetic in the temperature range from 30 to 200 K. This low T_C is fairly consistent with those of other $Zn_{1-x}Mn_xO$ films with high Mn concentration [13]. The magnetic behaviour of $Zn_{0.8}Mn_{0.2}O$ films is also confirmed by measuring the M–H curves at 5 K. The M–H curve of $Zn_{0.8}Mn_{0.2}O$ grown at 600 °C clearly shows a ferromagnetic hysteresis loop and the sample grown at 700 °C exhibits linear paramagnetic behaviour. The remanent magnetization and coercivity field value of the ferromagnetic $Zn_{0.8}Mn_{0.2}O$ film are 2.1 emu cm^{-3} and 570 Oe, respectively. These results suggest that the magnetic behaviour of the $Zn_{0.8}Mn_{0.2}O$ films is significantly affected by the growth temperature.

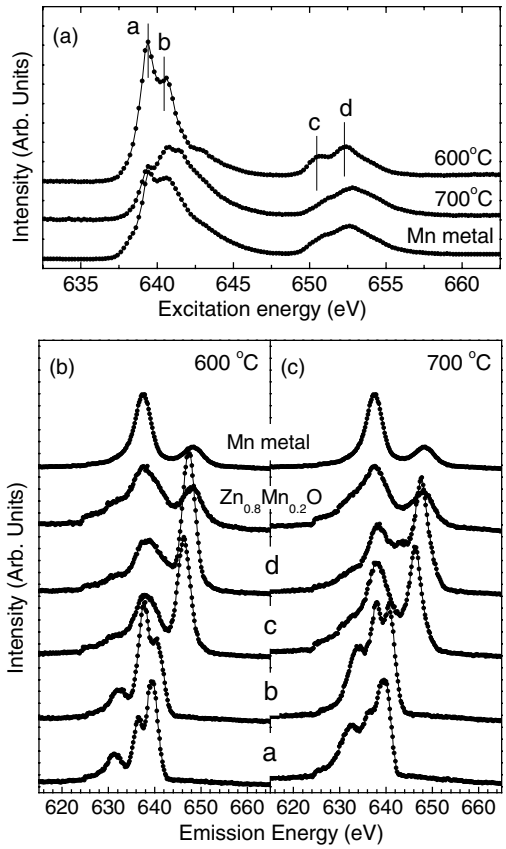

Figure 2. Mn $L_{2,3}$ x-ray absorption spectra of $Zn_{0.8}Mn_{0.2}O$ films and Mn metal (a) and resonantly excited Mn $L_{2,3}$ x-ray emission spectra of $Zn_{0.8}Mn_{0.2}O$ films grown at 600 °C (b) and 700 °C (c). The letters in (b) and (c) correspond to the excitation energies indicated in the XAS spectra (a). The nonresonant emission spectra of $Zn_{0.8}Mn_{0.2}O$ and Mn metal are shown in (b) and (c) for comparison.

The XRD patterns of the $Zn_{0.8}Mn_{0.2}O$ film grown at 600 and 700 °C are shown in figure 1(b). We observe a single (0002) peak at $2\theta = 34.2°$ for both samples, and the position of the (0002) peak does not change with elevated growth temperature. This reflects that the as-grown films have a high-quality wurtzite (B4) phase and the long-range ordering of $Zn_{0.8}Mn_{0.2}O$ does not depend on growth temperature, although the magnetic properties of $Zn_{0.8}Mn_{0.2}O$ films significantly depend on growth temperature. This is not surprising because the θ–2θ XRD scan tracks a line in k-space and cannot provide changes in the local structure around the Mn dopants or a possible formation of a secondary phase [10]. Similar magnetic behaviour with a dependence on growth temperature is also observed in 2 at.% Mn-doped ZnO when prepared using a sintering method. Sharma *et al* reported that Mn-doped ZnO pellets sintered below 600 °C are ferromagnetic at RT while samples sintered above 700 °C are paramagnetic [11]. They ascribed this suppression of ferromagnetism in Mn-doped ZnO at higher temperatures to the inhomogeneous distribution of Mn impurities that substitute for Zn sites.

Figure 2(a) shows the Mn $L_{2,3}$ XAS spectra of the ferromagnetic (FM) $Zn_{0.8}Mn_{0.2}O$ film (grown at 600 °C) and the nonmagnetic (non-FM) film (grown at 700 °C). The two main groups

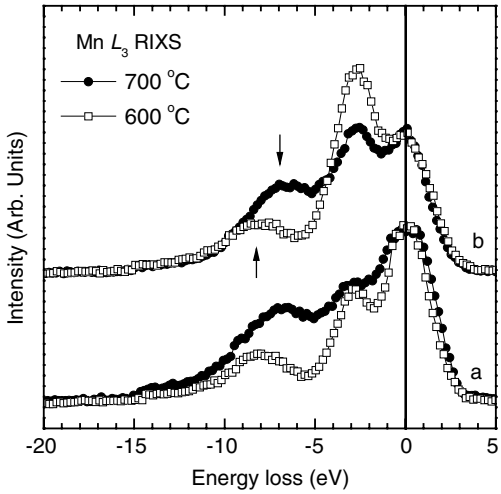

Figure 3. Resonant inelastic x-ray scattering spectra of $Zn_{0.8}Mn_{0.2}O$ films at the Mn L_3 edges. The spectra are plotted on energy loss scale and labels a and b correspond to the L_3 excitation energies of figures 2(b) and (c).

of Mn L_3 and Mn L_2 absorption lines are located around 640 eV and 651 eV respectively, and their energy separation is due to spin–orbit splitting of the 2p level. The Mn $L_{2,3}$ XAS spectrum of FM $Zn_{0.8}Mn_{0.2}O$ film exhibits multiplet features resulting from Coulomb and exchange interactions of the $2p^5$ core holes with the $3d^6$ electrons [14, 15]. The peak positions and the line shape are similar to those of MnO and MnS having Mn valences of 2+ and also for $Zn_{1-x}Mn_xO$ ($x = 0.015$–0.042) having Mn atoms substituted for Zn sites, but different from those of Mn_2O_3 and MnO_2 having trivalent (Mn^{3+}) and tetravalent Mn states (Mn^{4+}), respectively [16–18]. These results reflect that a FM $Zn_{0.8}Mn_{0.2}O$ film has the substitutional Mn^{2+} states in the T_d symmetry. On the other hand, Mn $2p_{3/2}$ and $2p_{1/2}$ absorption lines are broadened by elevating the growth temperature to 700 °C which is more typical for the itinerant Mn 3d states than for localized states.

To obtain the spectral information of occupied Mn 3d states from resonant inelastic x-ray scattering (RIXS) measurements, we chose four excitation energies, two at the L_3 threshold (spectra *a* and *b*) and two at the L_2 threshold (spectra *c* and *d*). The resulting RIXS spectra of $Zn_{0.8}Mn_{0.2}O$ films grown at 600 and 700 °C are displayed in figures 2(b) and (c). In addition, nonresonant x-ray emission spectroscopy (NXES) spectra excited at 665 eV are also included in the figures. The uppermost spectrum in each figure is the NXES spectrum of Mn metal. The overall spectral features exhibit a strong dependence on both excitation energy and growth temperature. The elastic peaks located at the same energies as those of the incident x-rays (639.3 and 640.5 eV) are shown in the spectra labelled *a* and *b*. The peak at 636.5 eV in the spectrum labelled *a* is attributed to dd excitations and follows the excitation energy. In order to evaluate the energy loss features, we plot the spectra *a* and *b* of both samples on the energy loss scale in figure 3. The dd excitation loss feature is located at about 3 eV below the elastic peak (at 0 eV). This feature corresponds to transitions to $3d^5$ multiplet states and is in good agreement with other measurements of MnO [15, 19].

In addition to the dd excitation loss, a weak structure appears below the dd loss, indicated by arrows. This feature shifts to a higher loss energy (about 8 eV) for the $Zn_{0.8}Mn_{0.2}O$ film grown at 600 °C. This relatively large energy loss is attributed to an interatomic charge transfer

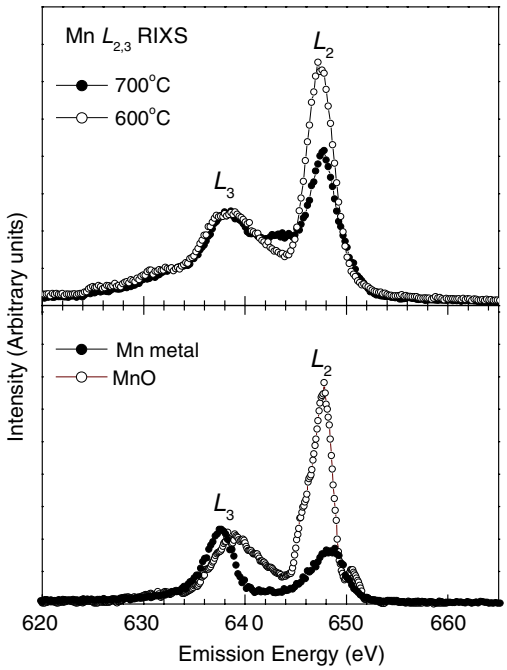

Figure 4. Resonant inelastic x-ray scattering spectra of $Zn_{0.8}Mn_{0.2}O$ films (a) and Mn metal and MnO excited at the Mn L_2 edge (652.3 eV).

excitation between the Mn atom and its nearest neighbour (oxygen in our case) because the Mn impurities in ZnO with a wurtzite structure substitute for Zn sites and thus are surrounded by oxygen neighbours. The energy and energy width of this peak are comparable to the $3d^6L$ configuration (L indicates a hole in the O 2p band) in MnO as reported by Butorin *et al* [15]. On the other hand, the loss peak shifts by about 1 eV toward the elastic peak for the non-FM $Zn_{0.8}Mn_{0.2}O$ film (grown at 700 °C). According to the XRD results, there is no lattice deformation upon increasing the growth temperature. Therefore the reduction of loss energy for the sample grown at 700 °C can only be explained by a change in the local surroundings of Mn impurities. This is in accordance with the Mn $L_{2,3}$ XAS spectra of the non-FM $Zn_{0.8}Mn_{0.2}O$ film which shows a more metallic feature than that of the FM sample. According to the electronic calculations reported by Máca *et al* [20], the interstitial Mn impurities in $Ga_{1-x}Mn_xAs$ have a higher local density of 3d occupied states near the Fermi level than the substitutional Mn atoms do. This is due to the enhanced hybridization that occurs with the close substitutional Mn neighbours.

The effect of elevated growth temperature on the interatomic interactions between Mn impurities and their neighbouring atoms can also be verified by comparing the spectral weight of the Mn L_2 emission line to that of the Mn L_3 line when exciting at the L_2 edge. This comparison is shown in figure 4(a). The intensity ratio of the Mn L_2 to the Mn L_3 emission line, $I(L_2)/I(L_3)$, of the non-FM $Zn_{0.8}Mn_{0.2}O$ film (700 °C) is much smaller than that of the FM $Zn_{0.8}Mn_{0.2}O$ film (600 °C). This reduction of spectral weight in L_2 with respect to L_3 for the non-FM $Mn_{0.8}Zn_{0.2}O$ film is largely due to radiationless Coster–Kronig (C–K) transitions. When x-ray transitions from (occupied) 3d4s valence states to $2p_{1/2}$ and $2p_{3/2}$ core holes occur in 3d transition metal solids, the $L_2L_3M_{4,5}$ C–K transitions depopulate the L_2 states of the system through radiationless transitions from L_2 to L_3 states before the normal emission

process takes place. The energy released in these transitions (11 eV for Mn 2p spin–orbit coupling in our case) promotes the emission of 3d Auger electrons. The suppression of the ratio $I(L_2)/I(L_3)$ due to C–K transitions is more prominent in metals (where there are more conduction electrons) than in insulating oxides [21, 22]. This is clearly seen in the Mn $L_{2,3}$ RIXS spectrum of Mn metal excited on the L_2 edge compared to that of insulating MnO as shown in figure 4(b).

Based on this information, one can see that the RIXS spectrum of the FM $Zn_{0.8}Mn_{0.2}O$ film resembles the spectrum of MnO in figure 4(a). According to electron paramagnetic resonance (EPR) measurements of $Zn_{1-x}Mn_xO$ [23], the Mn ions in the wurtzite ZnO crystal have a 2+ charge state and substitute for Zn sites. Hence the similar spectral feature of homogeneously distributed Mn dopant in ZnO to that in MnO is not unexpected. On the other hand, the non-FM $Zn_{0.8}Mn_{0.2}O$ film (700 °C) shows a limiting ratio between Mn metal and MnO, which suggests that direct Mn–Mn bonds form due to the precipitation of Mn atoms in ZnO that is induced by elevating the growth temperature. We conclude that the direct Mn–Mn antiferromagnetic exchange interaction suppresses the ferromagnetic ordering in the $Zn_{1-x}Mn_xO$ thin films. This effect seems to be especially significant in the system with a large Mn concentration and leads to a disappearance of ferromagnetism in the $Zn_{0.8}Mn_{0.2}O$ film.

4. Conclusions

To conclude, the local electronic structure of $Zn_{0.8}Mn_{0.2}O$ grown at different temperatures is studied using soft x-ray emission and absorption spectroscopy. Analysis of Mn $L_{2,3}$ emission spectra resonantly excited at the L_3 and L_2 edges reveals that the elevation of growth temperature induces direct Mn–Mn bonds due to the precipitation of Mn atoms in ZnO. This effect is absent in $Zn_{0.8}Mn_{0.2}O$ that is grown at a relatively low temperature. The RIXS technique as an element-specific and local probe offers a useful method for characterizing local environments around magnetic dopants in diluted magnetic semiconductors.

Acknowledgments

This work is supported by the Natural Sciences and Engineering Research Council of Canada (NSERC) and the Canada Research Chair programme. We gratefully acknowledge the Research Council of the President of the Russian Federation (Grants NSH-1026.2003.2), the Russian Science Foundation for Basic Research (Project 05-02-16438 and 05-02-17704), RFBR-Ural (Project 04-02-96096) and the National Creative Research Initiative Project, Korea.

References

[1] Ohno H 1998 *Science* **281** 951
[2] Dietl T, Ohno H, Matsukura F, Cibert J and Ferrand D 2000 *Science* **287** 1019
[3] Sato K and Katayama-Yoshida H 2000 *Japan. J. Appl. Phys.* **39** L555
[4] Sato K and Katayama-Yoshida H 2000 *Japan. J. Appl. Phys.* **40** L334
[5] Yamamoto T and Katayama-Yoshida H 1999 *Japan. J. Appl. Phys.* **38** L166
[6] Hu J and Gordon R G 1991 *Sol. Cells* **30** 437
[7] Minegishi K, Koiwai Y, Kikuchi Y, Yano K, Kasuga M and Shimizu A 1997 *Japan. J. Appl. Phys.* **36** L1453
[8] Joseph M, Tabata H, Saeki H, Ueda K and Kawai T 2001 *Physica* B **302/303** 140
[9] Look D C, Reynolds D C, Litton C W, Jones R L, Eason D B and Cantwell G 2002 *Appl. Phys. Lett.* **81** 1830
[10] Jung S W, An S-J, Yi G-C, Jung C U, Lee S-I and Cho S 2002 *Appl. Phys. Lett.* **80** 4561
[11] Sharma P, Gupta A, Rao K V, Owens F J, Sharma R, Ahuja R, Osorio Guillen J M, Johansson B and Gehring G A 2003 *Nat. Mater.* **2** 673

[12] Hong N H, Brizé V and Sakai J 2005 *Appl. Phys. Lett.* **86** 082505
[13] Janisch R, Gopal P and Spaldin N A 2005 *J. Phys.: Condens. Matter* **17** R657
[14] Arp U, Federmann F, Källen E, Sonntag B and Sorensen S L 1992 *J. Phys. B: At. Mol. Opt. Phys.* **25** 3747
[15] Butorin S M, Guo J-H, Magnuson M, Kuiper P and Nordgren J 1996 *Phys. Rev.* B **54** 4405
[16] Kang J-S, Kim G, Wi S C, Lee S S, Choi S, Cho S, Han S W, Kim K H, Song H J, Shin H J, Sekiyama A, Kasai S, Suga S and Min B I 2005 *Phys. Rev. Lett.* **94** 147202
[17] Okabayashi J, Ono K, Mizuguchi M, Oshima M, Gupta S S, Sarma D D, Mizokawa T, Fujimori A, Yuri M, Chen C T, Fukumura T, Kawasaki M and Koinuma H 2004 *J. Appl. Phys.* **95** 3573
[18] Kang J-S, Han S W, Park J-G, Wi S C, Lee S S, Kim G, Song H J, Shin H J, Jo W and Min B I 2005 *Phys. Rev.* B **71** 092405
[19] Jeng S-P and Henrich V E 1992 *Solid State Commun.* **82** 879
[20] Máca F and Mašek J 2002 *Phys. Rev.* B **65** 235209
[21] Grebennikov V I 2002 *Surf. Investigations: X-Ray, Synchrotron Neutron Tech.* **11** 41
[22] Kurmaev E Z, Ankudinov A L, Rehr J J, Finkelstein L D, Karimov P F and Moewes A 2005 *J. Electron Spectrosc. Relat. Phenom.* **148** 1
[23] Diaconu M, Schmidt H, Pöppl A, Böttcher R, Hoentsch J, Klunker A, Spemann D, Hochmuth H, Lorenz M and Grundmann M 2005 *Phys. Rev.* B **72** 085214